Carbohydrate Polymers 83 (2011) 1975–1983

Contents lists available at ScienceDirect

Carbohydrate Polymers

journal homepage: www.elsevier.com/locate/carbpol

Internal structures and phase-transitions of starch granules during gelatinization

Pei Chen [a,b,c,1], Long Yu [a,c,*], George P. Simon [b,**], Xingxun Liu [a,b,c], Katherine Dean [c], Ling Chen [a]

[a] Centre for Polymers from Renewable Resources, ERCPSP, School of Light Industry and Food, SCUT, Guangzhou, China
[b] Department of Materials Engineering, Monash University, Melbourne, Australia
[c] Commonwealth Scientific and Industrial Research Organization, CMSE, Melbourne, Australia

ARTICLE INFO

Article history:
Received 21 May 2010
Received in revised form 23 October 2010
Accepted 1 November 2010
Available online 9 November 2010

Keywords:
Starch
Microstructure
Phase transition
CLSM

ABSTRACT

The internal structures of corn starch granules with different amylose/amylopectin contents were studied using different microscopic techniques. The gelatinization phase transitions of the various starches were investigated by hot-stage confocal laser scanning microscopy (CLSM) and scanning electron microscopy (SEM). The influence of the amylose/amylopectin ratio on the internal structures and morphologies could be revealed by these techniques. Sharp growth ring structures could be clearly identified for high-amylopectin starches by CLSM and SEM following acid treatment. CLSM allowed the visualization of cross-sections of starch granules without the need for sectioning techniques that lead to destruction of the microstructure of sample, allowing exploration of the gelatinization mechanism. Three-dimensional images of starch granules during gelatinization could be constructed to further explore phase transition mechanisms. It was found that the granules of waxy maize and normal maize starch subsequently break through at their cavity and channels, when the granules became swollen during gelatinization, whilst the granules of G50 and G80 remain granular and break down to smaller pieces.

1. Introduction

It is well known that most native starches are a mixture of amylose (a linear structure of alpha-1,4 linked glucose units) and amylopectin (a highly branched structure of short alpha-1,4 chains linked with by alpha-1,6 bonds) (Zobel, 1984, 1988), and their ratio can vary over a very wide range, depending on their botanical origin. All starch granules contain both crystalline and amorphous regions, and are thus semi-crystalline, which in native starch granules manifests itself in a hierarchical structural periodicity which originates from the hilum (Blazek et al., 2009). The granules are organised into concentric rings radiating out from the central hilum to the surface of the granule. The number and size of the rings depend on the botanical origin of the starch, and it is generally believed to consist of alternating 120–400 nm thick amorphous and semi-crystalline growth rings (French, 1984). The amorphous growth rings contain both amylopectin and amylose macromolecules in relatively disordered conformations, whereas the semicrystalline growth rings consist of amylopectin clusters that contain alternating crystalline and amorphous regions of approximately 9–11 nm thickness, organised in a lamellar arrangement (Cameron & Donald, 1992; Kozlov, Noda, Bertoft, & Yuryev, 2006; Qi et al., 2004).

When the granules are subjected to treatment with dilute hydrochloric acid (Baker, Miles, & Helbert, 2001; Buttrose, 1963; Chen et al., 2009; Evers, McDermott, & Albans, 1970) or amylolytic enzymes (Planchot, Colonna, Gallant, & Bouchet, 1995), the ring structure becomes increasingly discernible (Yamaguchi, Kainuma, & French, 1979) and allowed the organization of the layered concentric shell structure of starch granules to be studied, such as by electron microscopy (SEM or TEM) or atomic force microscopy (AFM) of thin sections of granules or fragments of granules (Oostergetel & Van Bruggen, 1989; Ridout, Gunning, Parker, Wilson, & Morris, 2002; Yamaguchi et al., 1979). Blennow and colleagues (Blennow et al., 2003; Borén et al., 2008; Glaring, Koch, & Blennow, 2006) studied the ring structure of granular starch using CLMS after drying the samples using APTS (8-amino-1,3,6-pyrenetrisulfonic acid). Borén et al. (2008) have also compared the starch granules between Amo1 and its parental line Midas using CLMS, and found that the high-amylose content of the starch from Amo1 endosperm and visualized a noticeable degree of surface cracking of the granules. Recently Neethirajan, Thomson, Jayas, & White (2008) studied the surface of wheat starch granules by AFM and found thickness of layers was between 50 and 450 nm. In addition to the ring structure, channels extending from

* Corresponding author at: Commonwealth Scientific and Industrial Research Organization, CMSE, Melbourne, Australia. Tel.: +61 3 9545 2777; fax: +61 3 9544 1128.
** Corresponding author at: Monash University, Australia. Tel.: +61 3 9905 4936; fax: +61 3 9905 4934.
E-mail addresses: long.yu@csiro.au (L. Yu), george.simon@monash.edu.au (G.P. Simon).
[1] Present address: South China University of Agriculture, Guangzhou, China.

0144-8617/$ – see front matter © 2010 Elsevier Ltd. All rights reserved.
doi:10.1016/j.carbpol.2010.11.001

the outer surface to the centre of granule were also observed (Baldwin, Adler, Davies, & Melia, 1994; Gallant, Bouchet, & Baldwin, 1997).

The phase transitions of starch granules, particularly during the gelatinization process, are of both scientific and commercial importance (Liu, Xie, Yu, Chen, & Li, 2009). Starch gelatinization is irreversible and involves granular swelling, native crystalline melting, loss of birefringence and starch solubilization (Sullivan & Johnson, 1964) and has been extensively studied. Many different techniques have been developed to study the gelatinization in food and thermoplastics, for example, the estimation of maltose (Roberts, Potter, Kester, & Keneaster, 1954); determination of iodine blue complex (Roberts et al., 1954) and observation of polarizing patterns under microscope (Chen, Yu, Chen, & Li, 2006; Ghiasi and Hoseney (1982); Olkku & Rha, 1978; Tester & Morrison, 1992; Yeh & Li, 1996; Ziegler, 1993). In the last 20 years, differential scanning calorimetry (DSC) in particular has been widely used to study the thermal behaviour of starches, including gelatinization (Liu, Yu, Xie, & Chen, 2006; Yu & Christie, 2001). More recently, new methods to study the gelatinization under shear stress have been developed, such as RheoScope (Chen, Yu, Kealy, Chen, & Li, 2007; Yu, Kealy, & Chen, 2006), Haake Rheometer (Xue, Yu, Xie, Chen, & Li, 2008) and DMA (Xie, Yu, Chen, & Li, 2008). However, there is no technique that can directly observe the variation of internal section of starch granule and three-dimension of granule during gelatinization.

The aim of this work, therefore, is to further explore the inner microstructure conformation of the starch granules, especially the influence of the amylose/amylopectin ratio on the structure of the granule studied by scanning electronic microscopy (SEM) and confocal scanning laser microscopy (CLSM). In particular, CLSM allows direct observation of the variation of starch granule in three-dimensions, and is able to visualize cross-sections of starch granules without the need for sectioning techniques which can result in the destruction of the microstructure of sample. It can be highly instructive in the exploration of the gelatinization mechanism.

2. Experimental

2.1. Materials

Corn starches with different amylose/amylopectin ratios were used in the experimental work as model materials. All the starches are commercially available and were kindly supplied by Penford P/L (Australia). Gelose 50 and Gelose 80 are both corn starches, with amylose contents of 50% and 80%, respectively. Amylose contents in waxy maize and normal maize starches are 0% and 23% respectively.

8-Amino-1,3,6-pyrenetrisulfonic acid (APTS), sodium cyanoborohydride and HCl acid are highest purity, and were used as received from Sigma-Aldrich Corporation.

2.2. Sample preparation

2.2.1. Thermal treatment

A Linkam hot-stage apparatus used in microscopy was used to heat the starch suspensions. Each sample was heated from room temperature to the preset temperature at 2 °C/min, cooled to room temperature and observed under CLSM.

Starch samples were prepared for CLSM as previously described (Blennow et al., 2003). Starch granules (10 mg) were dispersed in 15 μl of freshly made APTS solution (10 mM APTS dissolved in 15% acetic acid) and 15 μl of 1 M sodium cyanoborohydride was added. The reaction mixture was incubated at 30 °C for 15–18 h, with the granules washed 5 times with 1 ml of distilled water and suspended in 20 μl of 1:1 (v/v) glycerol/water mixture. After dyeing the sample with APTS the starch suspension was sealed between two microscope glass slides using silicon adhesive.

2.2.2. Acid hydrolysis

Native starch was suspended in 4 M HCl (15 g of dry starch per 300 ml). The container was sealed with a lid and kept at room temperature for 5 days, with the suspension gently shaken daily to resuspend the sedimented granules. After hydrolysis, the insoluble residue was washed several times with distilled water to neutrality. The suspension was then filtered with Whatman No. 1 filter paper, with the acid-hydrolyzed starch dried at room temperature overnight under a stream of air.

2.3. Light microscopy

A polarization microscope (Axioskop 40 Pol/40 A Pol, ZEISS, Oberkochen, Germany) equipped with a 35 mm SLA camera was used in the experimental work. Iodine treatment was used to study internal structure of starch granules since iodine slips inside of the amylose coil and forming a deep blue color inclusion complex. 1 ml 5% starch suspensions were stained with 0.25 ml of a I2–KI dilute solution (2 mg/ml I2 + 20 mg/ml KI), and washed 20 min later with distilled water several times, and dispersed in a 1:1 (v/v) glycerol/water mixture to minimize evaporation and granule movement in the field before being examined with a light microscope, with both ordinary and polarized light used to investigate the morphology of the unstained starch.

2.4. Confocal laser scanning microscopy

A confocal laser scanning microscope equipped with an Ar/Hg laser (TCS SP2, Leica Microsystems, Wetzlar) and a stand for fixed fluorescent cell samples was used for the detection of the fluorescence signal from dye-stained starch granules. The details of the Leica objective lens used were: 100 × plan apo/1.40 oil UV. The excitation wavelength was 488 nm with 52 capacities, and the format of the image was 512 × 512. During image acquisition, each line was scanned four times and averaged in order to reduce noise.

For each starch sample a stack of horizontal optical sections was obtained, encompassing the whole starch granule in three dimensions. Measurements of the thickness of semi-crystalline ring of the granules were made with the software Imaris 6.1.5.

2.5. Scanning electronic microscope (SEM)

A small quantity of starch granules were embedded in epoxy, then poured into a tube mould. After curing for one night at room temperature these starch granules set in epoxy were held in liquid nitrogen for 3 min and cryo fractured for imaging. The sections were then immersed in 4 mol/L HCl solution at room temperature for 3 days, following which the sections were then rinsed three times for ten minutes with distilled water. These sections were dried at room temperature overnight under an air stream.

A Philips XL-30 FEGSEM SEM (scanning electronic microscope) was used to investigate the internal microstructure of starches. The air-dried starch powders were adhered to a specimen holder using a silver adhesive, and then coated with gold in a vacuum evaporator. The obtained specimens were viewed in the scanning electron microscope at an accelerating voltage of 2 kV.

3. Results and discussion

Fig. 1 shows the internal structures and morphologies of starch granules observed under the different microscopic techniques. Under brightfield optical microscopy, cracks were detected in the amylose-containing starch granules, this being enhanced when viewed under polarized light due to birefringence. Varying the amylose/amylopectin ratio does not result in a dramatic change

in the form of the birefringence pattern, although granular birefringence of the granules does decrease somewhat with increasing amylose content, resulting in a reduced contrast between birefringence and the background. This is expected since amylose molecules are not expected to be uniformly oriented in a specific direction (such as due to crystallization) in the granules. In contrast to the amylose-containing granules, the waxy maize granules almost keep similar color after treated with iodine revealing no amylose content. At the hilum core of amylose-containing granules, high local concentrations of amylose were detected (dark color). Similar phenomena have previously been reported by Blennow et al. (2003) for potato starch of different amylose contents.

CLSM optical and SEM cross-sections of different corn starches, with and without dyeing by APTS, are also showed in Fig. 1. It is seen that the APTS fluorescence intensity of amylose-rich starch is greater, which is expected since amylose has a much smaller molecule than amylopectin and contains a much higher molar ratio of reducing ends per anhydrous glucose residue than the amylopectin molecules, which results in a higher by-weight labeling of amylose (Blennow et al., 2003). The appearance of internal cavities in the starch granules could be clearly identified for different starches by CLSM after fluorescence labeling with APTS. SEM images confirmed that the cavities of these granules are voids, a similar phenomenon for potato starch having been reported by

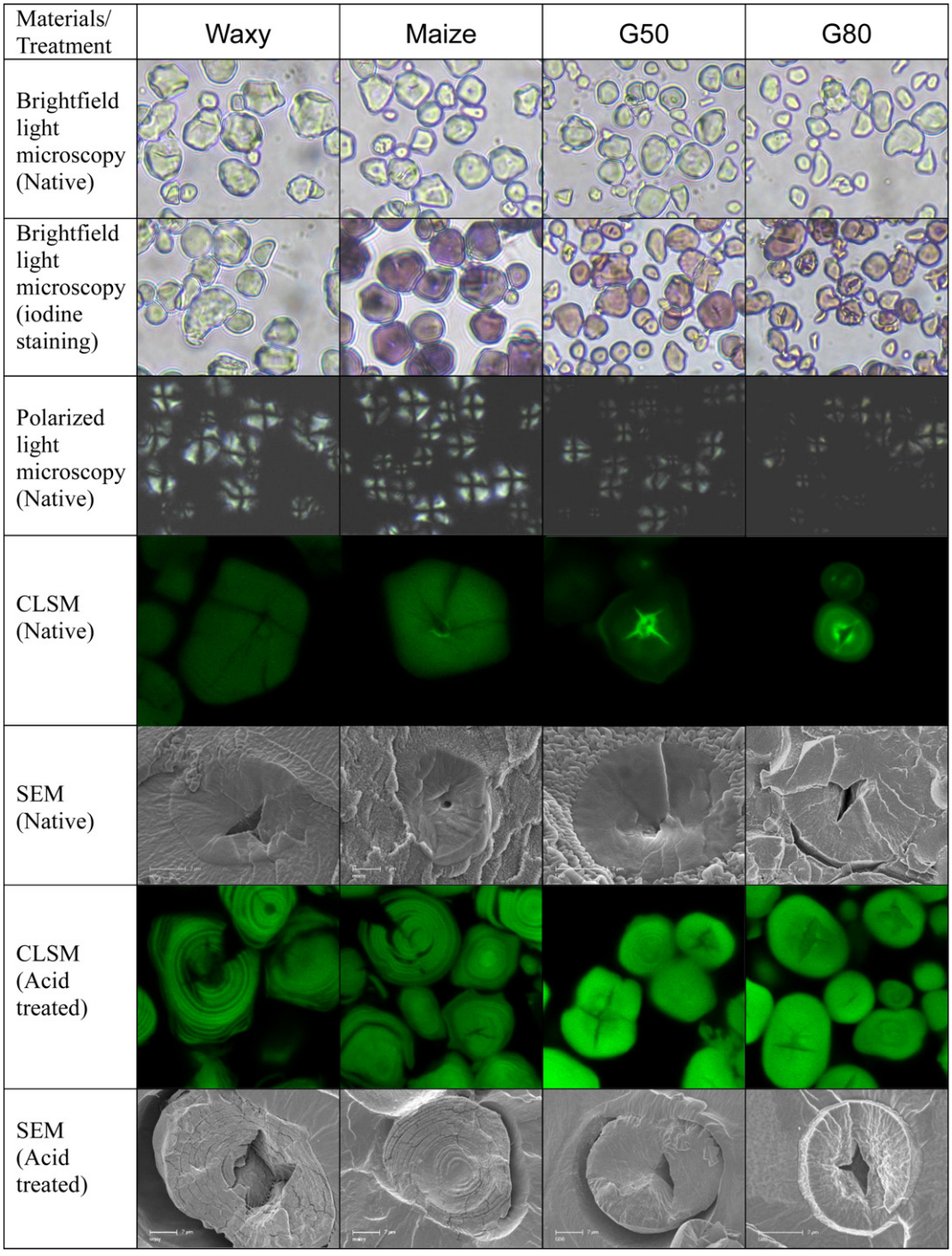

Fig. 1. Internal structures of different starches with and without treatment under different microscopes.

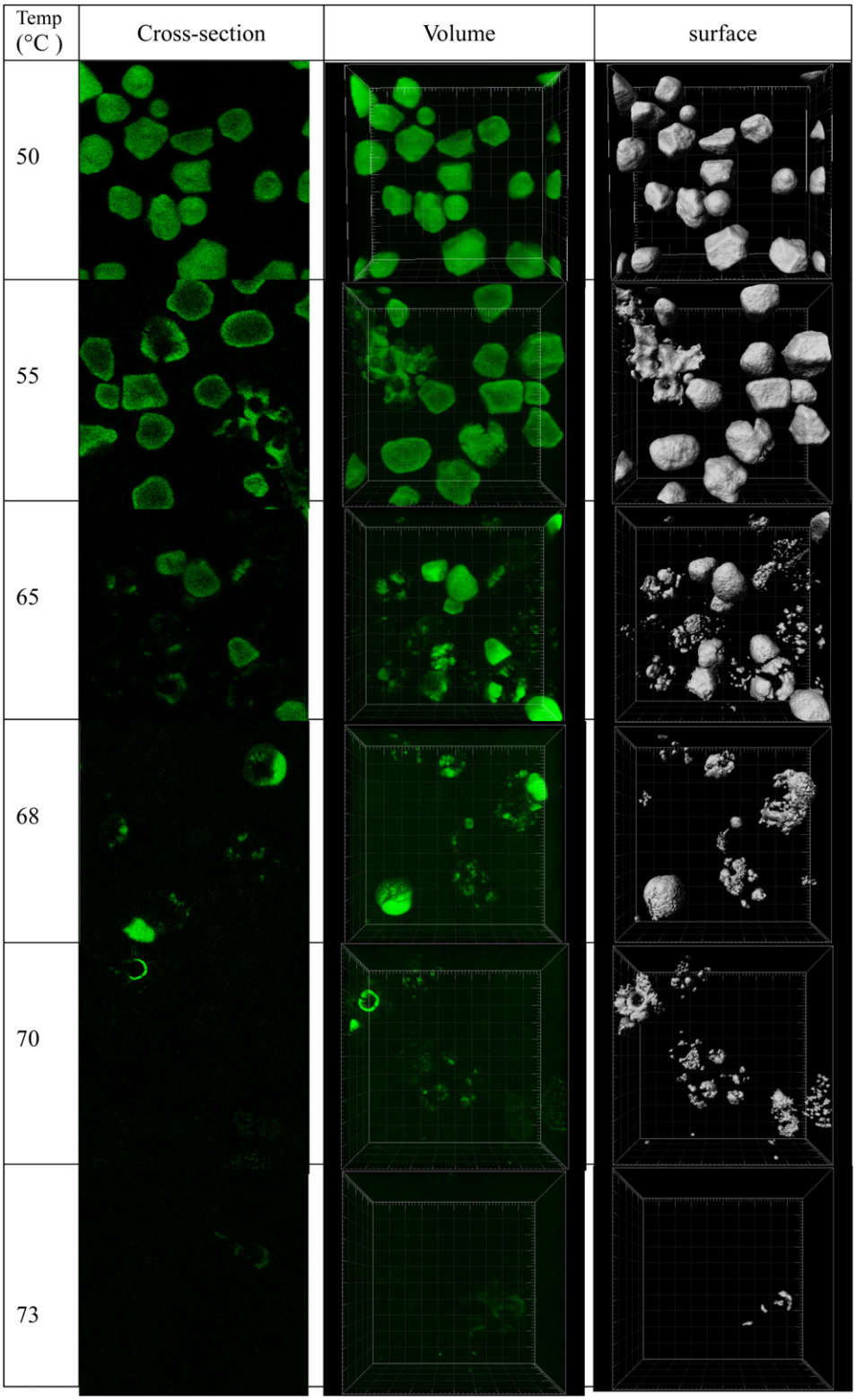

Fig. 2. Phase-transition of waxy maize starch at different temperatures by observed under CLSM.

Baldwin et al. (1994). Internal channels in starch granules can also observed under CLSM, and have been observed previously by SEM and CLSM (Huber & BeMiller, 2000; Kim & Huber, 2008). It can be seen that the channel structure differs significantly for the starches with different amylose content. More channels are observed in waxy maize and normal maize starch (low-amylose) than in the G50 and G80 (high-amylose), and these channels are more distinct. The channels were visible as dark lines running from the border of the granule toward the hilum in waxy maize and normal maize starch. In contrast, the channels show as a ring along the bright core in G50 and G80 starches. The channels of high amylose starch cannot be observed by SEM, which means they are not voids.

It is well known that the ratio of amylose and amylopectin in the starch granule leads to changes the relative sizes of the crystalline

Table 1
Average thickness of semi-crystalline growth rings for different corn starches.

Starch	Ratio of amylose/amylopectin	Growth rings (μm) obtained by CLSM	Growth rings (μm) obtained by SEM
Waxy	0/100	288	263
Maize	23/77	235	202
G50	50/50	NA	NA
G80	80/20	NA	NA

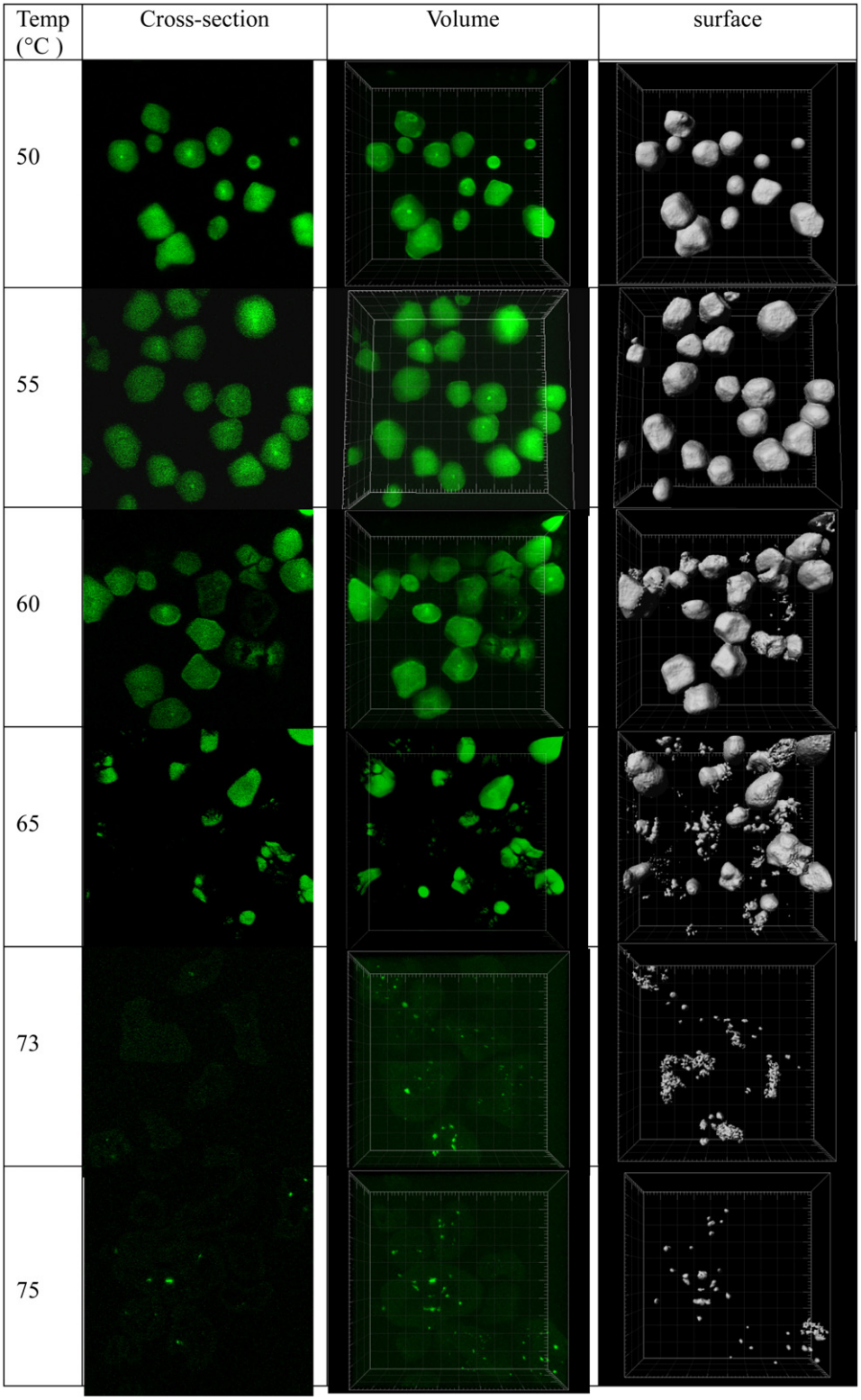

Fig. 3. Phase-transition of normal maize starch at different temperatures by observed under CLSM.

and amorphous areas (Jenkins & Donald, 1995). The understanding of the precise role of amylose content on the structure of the clusters, as well as on the sizes of semi-crystalline growth rings is still not fully understood. It is thus of interest to determine the influence of amylose content on the size of semi-crystalline growth rings, in particular for the same botanical source starches with different amylose content. However, the growth rings in starch granules are not visible under both CLSM and SEM cross-section images without further post-treatment. Acid treatment is an excellent way to reveal such a structure, since when granules are subjected to treatment with dilute hydrochloric acid the concentric layers becomes discernible due to a differential susceptibility to hydrolysis of parts of each layer (Evers et al., 1970). The strong fluorescence of such hydrolyzed starch granules demonstrated that the increase of reac-

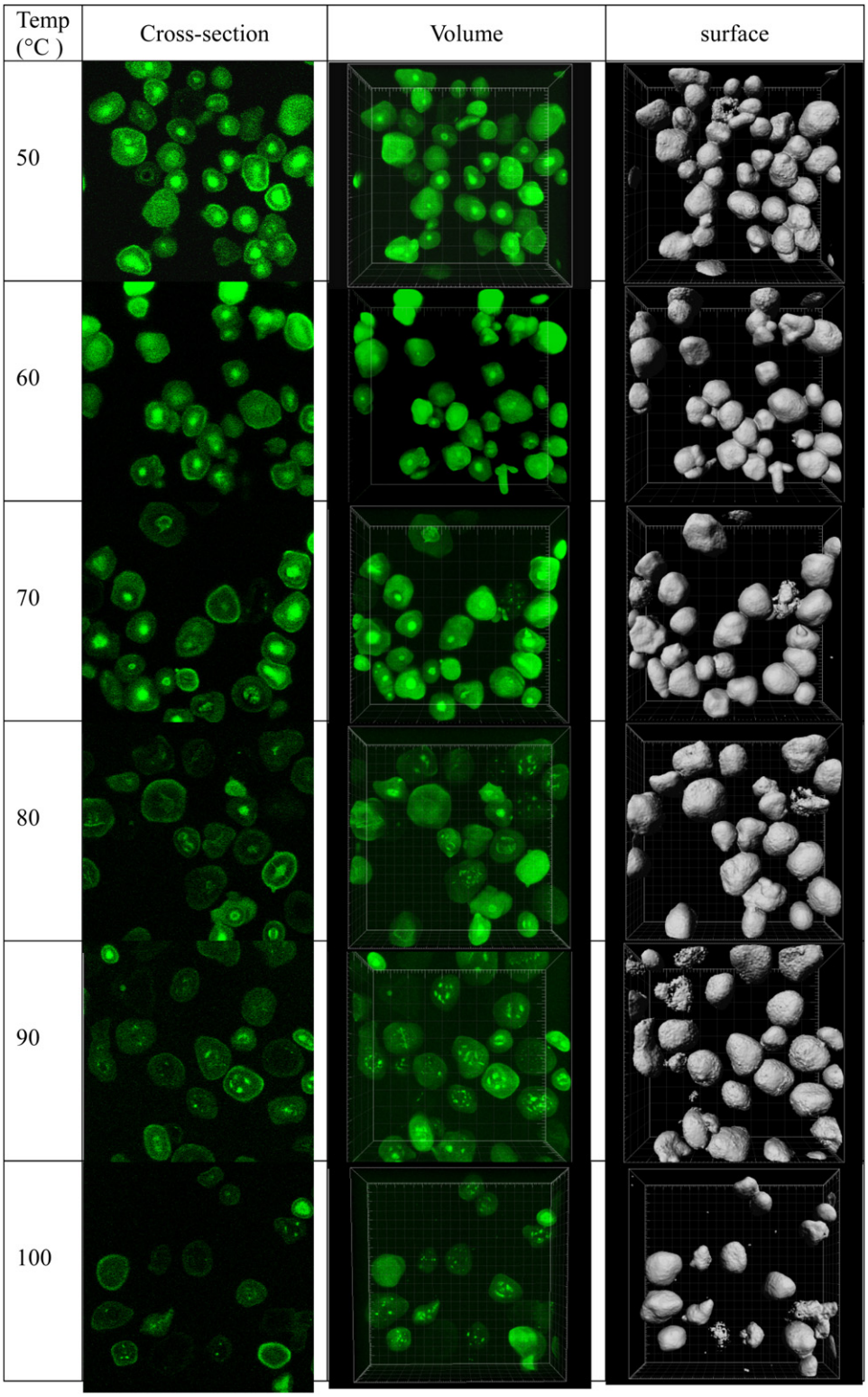

Fig. 4. Phase-transition of G50 starch at different temperatures observed by under CLSM.

tion end after hydrolysis which reacted with more APTS molecules (compare the native and treated starch granules under CMSM). A possible explanation is that the acid hydrolysis attacked the amorphous region first, leading to better contrast between amorphous and semicrystalline layers within the starch granules. After the acid treatment, amorphous rings have been removed and the image contract of semicrystalline rings has been enhanced by the increase of reaction end. Chung and Lai (2006) reported that corn starch treated with HCl-methanol increased both fluorescence intensity and the clear growth rings under CLSM. Both CLSM and SEM images of the corn starches after acid hydrolysis are presented in Fig. 1. Alternating light and dark layers are observed in waxy maize and normal maize starch, the former being related to semi-crystalline growth rings, with the latter ascribed to the amorphous background

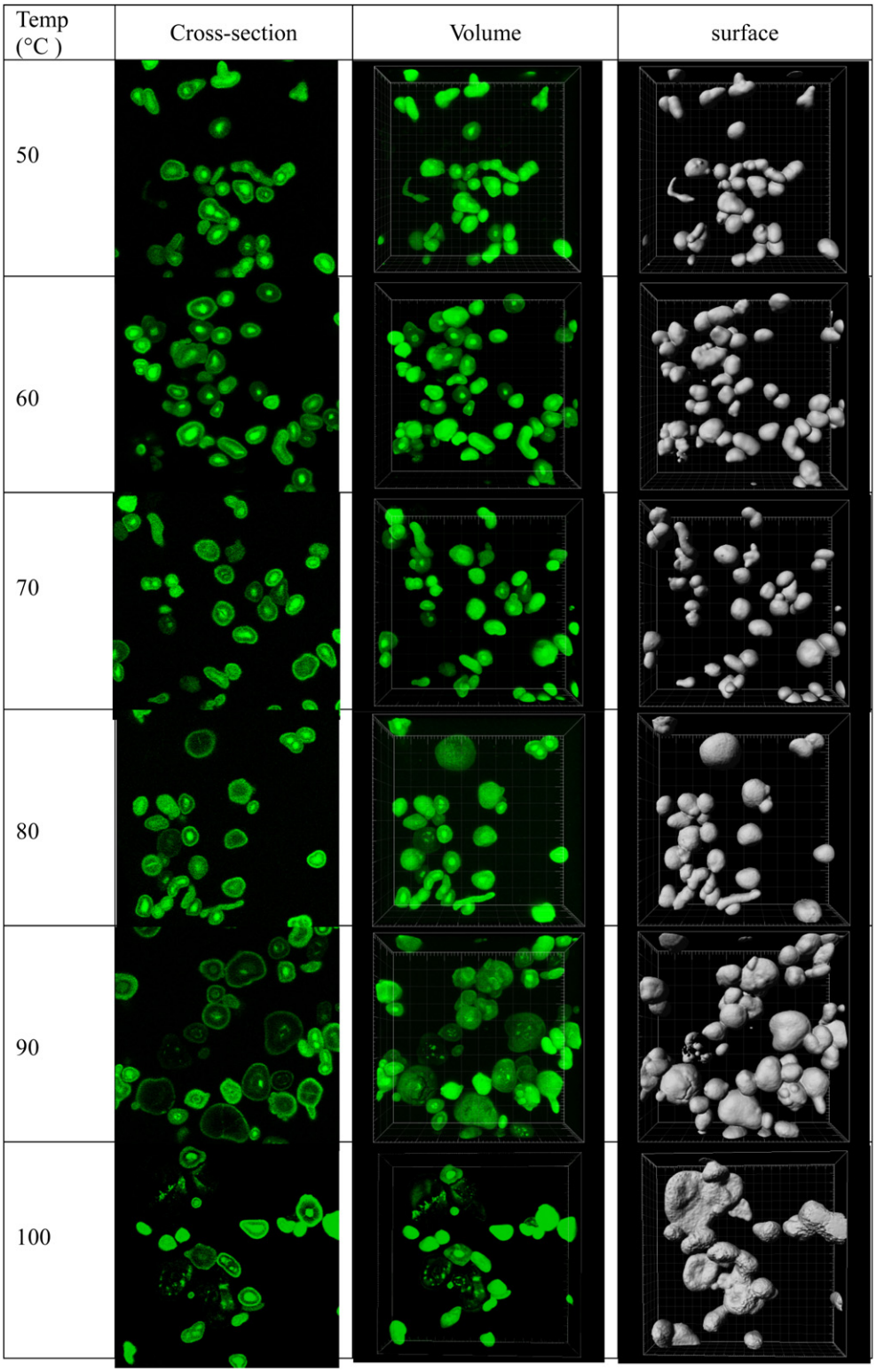

Fig. 5. Phase-transition of G80 starch at different temperatures, observed by under CLSM.

(Yuryev et al., 2004). No growth rings were observed in G50 and G80, and the holes in the hilum were bigger in the higher amylose-containing starches.

As previously reported (Chen et al., 2006), waxy maize and normal maize starch show typical A-type patterns, whilst G50 and G80 showed B-type patterns. B-type starches are known to be more resistant to acid hydrolysis than A-type starches. Acid hydrolyzed starch granules broke down at a progressively more rapid rate, as the amylose content decreases. Over the broad range of amylose content, three main factors are considered to influence the structural parameters of native starch granules at the nanoscale: (i) amylose defects located in the crystalline region of the lamellae (both as amylose tie-chains and amylose–lipid complexes), (ii) the amount of amylose within the amorphous regions of the lamellae, and (iii) chain length distribution of amylopectin chains (Blazek et al., 2009; Kozlov et al., 2007). Detailed analysis of the CLSM and SEM photographs reveal that the average thickness of semi-crystalline growth rings of waxy maize are slightly higher than normal maize starch (see Table 1), whilst no growth rings can be observed in high amylose starch (G50 and G80). This phenomenon is different from the observation for wheat starches (Yuryev et al., 2004), which showed that the average thickness of semi-crystalline growth rings increased with increasing amylose content.

Figs. 2–5 show the morphological variations of different starches during heating, as observed under CLSM, and mainly represent the critical points in structural change. For each sample, a stack of horizontal optical sections was obtained, encompassing the whole starch granule in three dimensions. The first column shows the cross-section of starch granules. The second and third column show the three-dimensional images based on volume and surface sections, respectively. The 3D images of starch granules and in particular the images based on surface sections, are similar to those observed from SEM. The advantage of 3D images from CLSM is that it can observe the phase transition during gelatinization. In comparison, SEM cannot be used to view a sample of starch suspended in water, whilst other optical microscope techniques are not able to "slice" the object and construct such a instructive 3D image.

It can be seen that the diameter of granules increased with increasing temperature for all starches, whilst brightness of all starches decreased, and the decreasing started from centre of granule. It is expected that since the central area of the granule around the hilum is the least organized region, modification due to both acid hydrolysis and (in particular) gelatinization will commence from this point. It was observed that fluorescence remained at granule surface for low amylose starch (waxy maize and normal maize starch), whilst bright cores were observed for high amylose starch (G50 and G80) during gelatinization.

The temperatures at which the bright granules disappeared are significantly different for the different starches, disappearing at lower temperatures for the amylopectin richer starches. The disappearance of bright starch structures occurs at temperatures of about 70 and 73 °C for waxy maize and normal maize starch, whilst the bright granule of high amylose starches (G50 and G80) are still clearly observed at 100 °C – the highest temperature attainable in this work. These phenomena are similar to imaging, which make use of the birefringence variation of starch granules observed under polarized light (Chen et al., 2006). It needs to be noted that generally the APTS stains equimolar, i.e. mostly, if not entirely amylose is detected, which did not affect the compression results.

Corresponding to the disappearance of brightness, the process of granule breaking and disappearance can be observed by 3D images. The granules of waxy maize and normal maize disappeared the cavity and channels when the granules became swollen during gelatinization, whilst the granules of G50 and G80 remain in a granular form. Indeed, the granules of the waxy maize and normal maize starch start to break into small pieces at temperature at about 55 and 60 °C, respectively, and are totally destroyed at about 73 and 75 °C. The granules of G50 and G80 remained in spherulitic form up to 100 °C – the maximum temperature investigated in this work.

4. Conclusions

Different microscopic techniques were used to study the internal structural characteristics of corn starches with different amylose/amylopectin contents, both in terms of internal structure and morphology. CLSM proved to be an effect research tool for the exploration of the internal structure of starch granules. Sharp growth ring structures were clearly revealed in low-amylose starches (waxy maize and normal maize), when modified by acid hydrolysis. Conversely, no growth rings were found in high amylose starches (G50 and G80), even following such treatment.

The change in morphology of the different starches during heating was studied using CLSM. For each sample, a stack of horizontal optical sections was obtained, encompassing the whole starch granule in three dimensions. Brightness of starch granule indicates the degree of gelatinization. The brightness of all the starches decreased with increasing temperature, this change being initiated at the centre of granule. Thus it is clear that the gelatinization process starts at the hilum of the granules. The central area of the granule around the hilum is believed to be the least organized region, since both gelatinization and acid hydrolysis initiate at this region. The granules of waxy maize and normal maize starch subsequently break through at their cavity and channels, when the granules became swollen during gelatinization, whilst the granules of G50 and G80 remain granular and break down to smaller pieces.

Acknowledgements

The authors from SCUT, China, would like to acknowledge the research funds NRDPHT (863) (2007AA10Z312, 2007AA100407), NKTRDP (2006BAD27B04) and ASTATFP (2009GB23600523). We would like to acknowledge Monash Micro Imaging for the CLSM for this work. P. Chen and X. Liu would like to knowledge the State Scholarship Fund provided by China Scholarship Council supports her study in Australia.

References

Baker, A. A., Miles, M. J., & Helbert, W. (2001). Internal structure of the starch granule revealed by AFM. *Carbohydrate Research*, *330*, 249–256.

Baldwin, P. M., Adler, J., Davies, M. C., & Melia, C. D. (1994). Holes in starch granules: confocal SEM and light microscopy studies of starch granule structure. *Starch/Stärke*, *46*, 341–346.

Blazek, J., Salman, H., Rubio, A. L., Gilbert, E., Hanley, T., & Copeland, L. (2009). Structural characterization of wheat starch granules differing in amylose content and functional characteristics. *Carbohydrate Polymers*, *75*, 705–711.

Blennow, A., Hansen, M., Schulz, A., Jorgensen, K., Donald, A. M., & Sanderson, J. (2003). The molecular deposition of transgenically modified starch in the starch granule as imaged by functional microscopy. *Journal of Structural Biology*, *143*, 229–241.

Borén, M., Glaring, M., Ghebremedhin, H., Olsson, H., Blennow, A., & Jansson, C. (2008). Molecular and physicochemical characterization of the high-amylose barley mutant Amo1. *Journal of Cereal Science*, *47*, 79–89.

Buttrose, M. S. (1963). Electron-microscopy of acid-degraded starch granules. *Starch/Stärke*, *15*, 85–92.

Cameron, R. E., & Donald, A. M. (1992). A small-angle X-ray scattering study of the annealing and gelatinization of starch. *Polymer*, *33*, 2628–2635.

Chen, P., Yu, L., Chen, L., & Li, X. (2006). Morphology and microstructure of maize starches with different amylose/amylopectin content. *Starch/Stärke*, *58*, 611–615.

Chen, P., Yu, L., Kealy, T., Chen, L., & Li, L. (2007). Phase transition of starch granules observed by microscope under shearless and shear conditions. *Carbohydrate Polymers*, *68*, 495–501.

Chen, P., Yu, L., Simon, G., Petinakis, E., Dean, K., & Chen, L. (2009). Morphologies and microstructures of corn starches with different amylose-amylopectin ratios studied by confocal laser scanning microscope. *Journal of Cereal Science*, *50*, 241–247.

Chung, Y. L., & Lai, H. M. (2006). Molecular and granular characteristics of corn starch modified by HCl–methanol at different temperatures. *Carbohydrate Polymers*, *63*, 527–524.

Evers, A. D., McDermott, E. E., & Albans, S. (1970). Scanning electron microscopy of wheat starch II. Structure of granules modified by alpha-amylolysis – Preliminary report. *Starch/Stärke*, *22*, 22–26.

French, D. (1984). Organization of starch granules. In R. L. Whistler, J. N. Bemiller, & E. F. Parschall (Eds.), *Starch, chemistry and technology* (pp. 183–247). New York: Academic Press.

Gallant, D. J., Bouchet, B., & Baldwin, P. M. (1997). Microscopy of starch: evidence of a new level of granule organization. *Carbohydrate Polymers*, *32*, 177–191.

Ghiasi, K., & Hoseney, R. C. (1982). Varriano-Marston E. Gelatinization of wheat starch: 3 – Comparison by differential scanning calorimetry and light microscopy. *Cereal Chemistry*, *59*, 258–262.

Glaring, M., Koch, C., & Blennow, A. (2006). Genotype-specific spatial distribution of starch molecules in the starch granule: A combined CLSM and SEM approach. *Biomacromolecules*, *7*, 2310–2320.

Huber, K. C., & BeMiller, J. N. (2000). Channels of normal maize and sorghum starch granules. *Carbohydrate Polymers*, *41*, 269–276.

Jenkins, P. J., & Donald, A. M. (1995). The influence of amylose on starch granule structure. *International Journal of Biological Macromolecules*, *17*, 315–321.

Kim, H.-S., & Huber, K. C. (2008). Channels within soft wheat starch A- and B-type granules. *Journal of Cereal Science*, *48*, 159–172.

Kozlov, S. S., Noda, T., Bertoft, E., & Yuryev, V. P. (2006). Structure of starches extracted from near isogenic wheat lines – Part I. Effect of different GBSS I combinations. *Journal of Thermal Analysis and Calorimetry*, *86*, 291–301.

Kozlov, S., Krivandin, A., Shatalova, O., Noda, T., Bertoft, E., Fornal, J., et al. (2007). Structure of starches extracted from near-isogenic wheat lines. *Journal of Thermal Analysis and Calorimetry*, *87*, 575–584.

Liu, H., Yu, L., Xie, F., & Chen, L. (2006). Gelatinization of cornstarch with different amylose/amylopectin content. *Carbohydrate Polymers*, *65*, 357–363.

Liu, H., Xie, F., Yu, L., Chen, L., & Li, L. (2009). Thermal processing of starch-based polymers. *Progress in Polymer Science*, *34*, 1348–1368.

Neethirajan, S., Thomson, D. J., Jayas, D. S., & White, N. D. G. (2008). Characterization of the surface morphology of durum wheat starch granules using atomic force microscopy. *Microscopy Research and Technique*, *71*, 125–132.

Olkku, J., & Rha, C. (1978). Gelatinization of starch and wheat flour starch – A review. *Food Chemistry*, *32*, 293–317.

Oostergetel, T. G., & Van Bruggen, J. E. (1989). On the origin of a low angle spacing in starch. *Starch/Stärke*, *41*, 331–335.

Planchot, V., Colonna, P., Gallant, D. J., & Bouchet, B. (1995). Extensive degradation of native starch granules by alpha-amylase from aspergillus fumigatus. *Journal of Cereal Science*, *21*, 163–171.

Qi, X., Tester, R. F., Snape, C. E., Yuryev, V., Wasserman, L. A., & Ansell, R. (2004). Molecular basis of the gelatinisation and swelling characteristics of waxy barley starches grown in the same location during the same season. Part II. Crystallinity and gelatinisation characteristics. *Journal of Cereal Science*, *39*, 57–66.

Ridout, M. J., Gunning, A. P., Parker, M. L., Wilson, R. H., & Morris, V. J. (2002). Using AFM to image the internal structure of starch granules. *Carbohydrate Polymers*, *50*, 123–132.

Roberts, R. L., Potter, E. L., Kester, E. B., & Keneaster, K. K. (1954). Effect of processing conditions on the expanded volume, color, and soluble starch of parboiled rice. *Cereal Chemistry*, *31*, 121–125.

Sullivan, J. W., & Johnson, J. A. (1964). Measurement of starch gelatinization by enzyme susceptibility. *Cereal Chemistry*, *41*, 73–77.

Tester, R. F., & Morrison, W. R. (1992). Swelling and gelatinization of cereal starches: III — Some properties of waxy and normal nonwaxy barley starches. *Cereal Chemistry*, *69*, 654–658.

Xie, F., Yu, L., Chen, L., & Li, L. (2008). A new study of starch gelatinization under shear stress using dynamic mechanical analysis. *Carbohydrate Polymers*, *72*, 229–234.

Xue, T., Yu, L., Xie, F., Chen, L., & Li, L. (2008). Rheological properties and phase transitions of starch under shear stress. *Food Hydrocolloids*, *22*, 973–978.

Yamaguchi, M., Kainuma, K., & French, D. (1979). Electron microscopic observations of waxy normal maize starch. *Journal of Ultrastructure Research*, *69*, 249–261.

Yeh, A.-I., & Li, J.-Y. (1996). A continuous measurement of swelling of rice starch during heating. *Journal of Cereal Science*, *23*, 277–283.

Yu, L., & Christie, G. (2001). Measurement of starch thermal transitions using differential scanning calorimetry. *Carbohydrate Polymers*, *46*, 179–184.

Yu, L., Kealy, T., & Chen, P. (2006). Study of starch gelatinization in a flow field using simultaneous rheometric data collection and microscopic observation. *International Polymer Processing*, *3*, 283–289.

Yuryev, V. P., Krivandin, A. V., Kiseleva, V. I., Wasserman, L. A., Genkina, N. K., Fornal, J., et al. (2004). Structural parameters of amylopectin clusters and semi-crystalline growth rings in wheat starches with different amylose content. *Carbohydrate Research*, *339*, 2683–2691.

Ziegler, G. R., Thompson, D. B., & Casasnovas, J. (1993). Dynamic measurement of starch granule swelling during gelatinization. *Cereal Chemistry*, *70*, 247–251.

Zobel, H. F. (1984). R. L. Whistler (Ed.), *Starch: chemistry and technology* London: Academic Press.

Zobel, H. F. (1988). Molecules to granules: A comprehensive starch review. *Starch/Stärke*, *40*, 44–50.